

Fig. 4. Normalized susceptance for a negative capacitor in uniformly loaded waveguide.

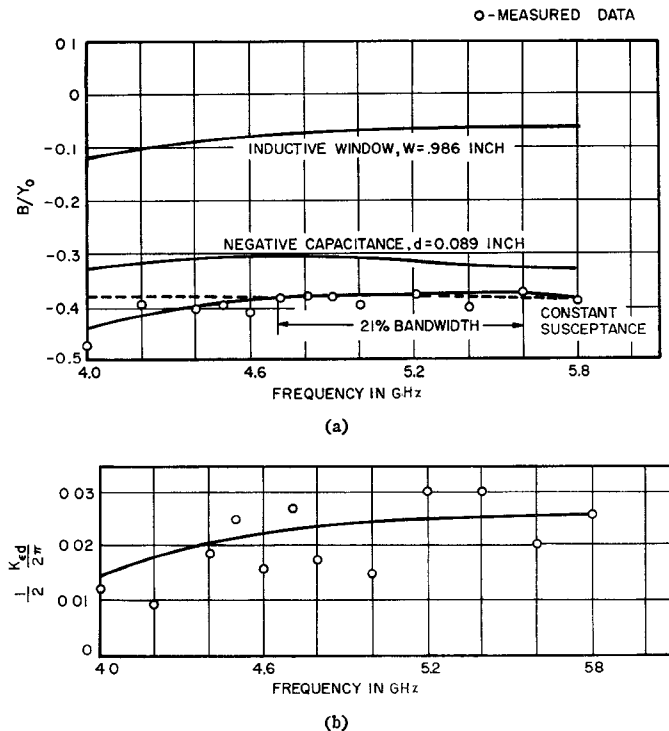


Fig. 5. Equivalent circuit parameters for experimental constant susceptance network. (a) Normalized susceptance. (b) Normalized line length.

erated, and relatively good experimental agreement obtained. Fig. 4 is a plot of the normalized susceptance of the negative capacitance in waveguide. The susceptance of an inductive iris has the same algebraic sign as that of the negative capacitor, but at frequencies greater than  $\sqrt{2}f_c$  their frequency trends are opposite. When the slopes of the two elements are equal in magnitude, the magnitude of the inductive susceptance will be about one-fourth the magnitude of the negative-capacitive susceptance. Consequently, it seems reasonable that the introduction of a small inductive perturbation of proper magnitude into the window would produce a constant susceptance. Moreover, it is assumed that the total susceptance can be obtained by determining the susceptance of the inductive iris in the absence of the window, and adding this to the susceptance of the negative capacitance. This is particularly well founded since the iris perturbs the modal  $H$  field, which is not affected by the presence of the window, and the window provides a discontinuity to the modal  $E$  field, which is not significantly affected by the iris,

Consequently using Marcuvitz's formula for the susceptance of the iris,<sup>3</sup> the formula for the total normalized susceptance is obtained

$$\frac{B_t}{Y_0} = -\frac{\lambda_1}{a} \cot^2 \frac{\pi w}{2a} - \frac{2\pi d \lambda_1}{\lambda^2} (\epsilon_1 - \epsilon_2). \quad (6)$$

The validity of (6) was experimentally determined by measuring the impedance of a constant susceptance network in polystyrene ( $\epsilon_1 = 2.56$ ) loaded WR112 waveguide. The length of the window was 0.089 inch, while  $\epsilon_2$  was unity. The iris aperture  $w$  was 0.986 inch. These values were determined by equating the values of (6) for 4.7 and 5.8 GHz. The nominal susceptance, over the 21 percent band, for these parameters is 0.375. Fig. 5 shows curves of the computed circuit parameters and measured data.

ALEXANDER J. KELLY  
Airborne Instrument Lab.  
Div. of Cutler-Hammer, Inc.  
Melville, L. I., N. Y.

<sup>3</sup> N. Marcuvitz, *Waveguide Handbook*, Rad. Lab. Ser., vol. 10. New York: McGraw-Hill, 1950, p. 221.

## High-Power S-Band Power Divider

The problem of covering the full power range from milliwatts to megawatts in laboratory experiments, with a minimum number of RF power source, and instrumentation changes, has always existed in the field of microwaves. A high-power attenuator, covering a 20 or 30 dB power range using a single RF power source, is needed so that experiments can yield more complete data. The power source used could be set to a fixed frequency and output power level, and the attenuator could be adjusted to supply discrete amounts of power, as needed, to test an experimental device. The frequency of the power source would not have to be readjusted each time the power out of the attenuator is changed.

Since an in-line attenuator must absorb all of the energy it does not pass, it is automatically power limited. However, a power divider diverts the unused portion of the RF energy to an external dummy load. Since the power absorbed by the power divider itself is negligible, the only design problems are those of high-voltage breakdown and impedance matching.

The power divider discussed here provides a 30 dB dynamic range of power control and a peak power handling capability of at least 700 kilowatts at S band. A high peak power rating is necessary because there are some pulsed magnetrons that must operate at a minimum of 300 to 400 kilowatts in order to produce a stable output with a satisfactory pulse shape. A magnetron usually provides satisfactory operation over a dynamic power range of only 6 to 8 dB.

The power divider consists basically of four units: 1) an input-output adapter section, 2) a 3 dB hybrid coupler, 3) a dual waveguide shutter assembly, and 4) a sidewall "panty" adapter (so called because of its unique shape). A pair of matched loads are also used, but they are external to the power divider. A block diagram of the power divider is shown in Fig. 1.

The input RF power from a magnetron or other high-power source is fed through the input arm of the input-output adapter section and into the 3 dB hybrid coupler. The RF input power, fed into port 1, splits into two equal amounts of power that pass out of ports 2 and 3, respectively. These two RF signals, which we shall designate as signals  $A$  and  $B$ , pass through the panty adapter and enter the RF dual shutter assembly.

The RF dual shutter assembly is constructed so that both halves of the shutter open and close in unison. If the shutters are both completely open, then all of signal  $A$  is absorbed as signal  $A1$  by matched load  $A$ . Likewise, all of signal  $B$  is absorbed as signal  $B1$  by matched load  $B$ . When the shutters are completely closed, then all of signals  $A$  and  $B$  are reflected as  $A2$  and  $B2$ . Whenever the shutters are partially open, equal amounts of signals  $A$  and  $B$  are reflected.

The output power at port 4 will be equal to the sum of signals  $A2$  and  $B2$ . Signal  $A2$  leads signal  $B2$  by 90 degrees at the input to the hybrid coupler, but signal  $B2$  will receive a 90 degree phase lead going through the hybrid coupler from port 3 to port 4. As a

Manuscript received November 11, 1966; revised May 17, 1967.

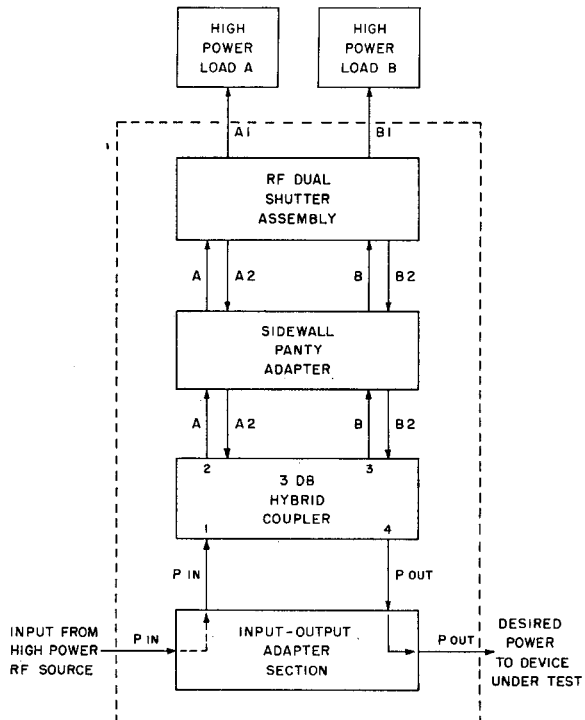


Fig. 1. Block diagram of high-power power divider.

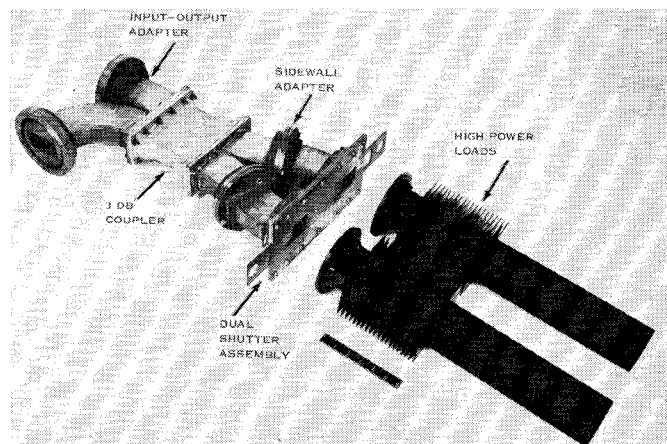


Fig. 2. Complete power divider.

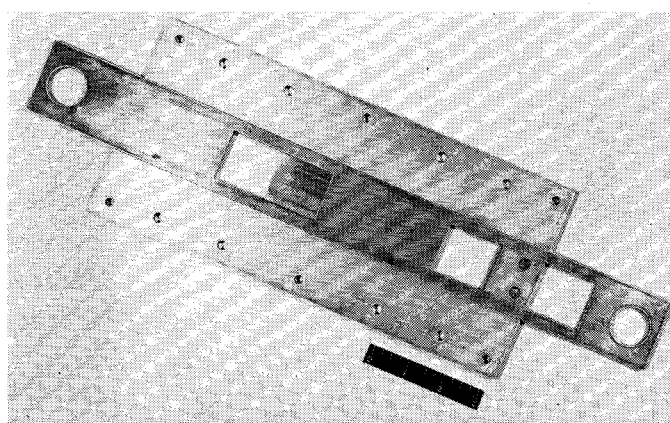


Fig. 3. RF shutters in half-closed position.

result, signals  $A2$  and  $B2$  will combine in phase at port 4 of the hybrid coupler. This RF signal will pass through the input-output adapter to the device under test. The amount by which the input power can be attenuated is limited only by the isolation of the 3 dB hybrid coupler, which determines the amount of leakage power from port 1 to port 4, and by the VSWR of the high-power loads. A hybrid coupler isolation of greater than 30 dB will produce a dynamic range of operation of approximately 30 dB with any reasonably well-matched (VSWR of 1.05 or less) high-power loads.

Fig. 2 is a photograph of the complete power divider assembly, including a pair of matched loads. The input-output adapter was formed by joining a 90 degree  $H$ -plane bend and a straight waveguide section together in a dual side-wall flange. This adapter mates the standard round flanged components to the dual side-wall flange on the 3 dB hybrid coupler.

The complete assembly (shown in Fig. 2) is  $4\frac{1}{2}$  inches long by  $5\frac{7}{16}$  inches wide by  $17\frac{5}{8}$  inches high. The power divider assembly is only  $22\frac{1}{2}$  inches long, while the dummy loads take up the remaining 20 inches of length. A "panty" fitting was constructed by making two offsets from two pairs of  $22\frac{1}{2}$  degree  $H$ -plane bends and joining the two assemblies at one end in a dual side-wall flange, which mates to the 3 dB hybrid coupler. The two output legs of this assembly are  $3\frac{1}{4}$  inches apart. The minimum offset spacing for proper operation is 3 inches, since the total shutter travel is equal to the 2.84 inch distance across the inside of the RG-48 waveguide.

The 3 dB hybrid coupler is a commercially available, cast aluminum unit with a frequency range of 2.99 to 3.44 GHz. It has an isolation characteristic of over 30 dB and a coupling value of  $3\text{ dB} \pm 0.1\text{ dB}$  over the specified frequency range. If a different range of S-band frequencies is desired, the power divider can be modified merely by changing the accompanying hybrid coupler. The 3 dB hybrid coupler is the only frequency-sensitive component in the power divider, and its isolation characteristic at the operating frequency will determine the dynamic range of the power divider. The high-power loads will be relatively frequency independent provided they are reasonably well matched and have a low VSWR. The loads used with this power divider are each capable of handling at least 500 watts of average power.

The dual RF shutter assembly was machined from three brass plates of standard thickness. The shutter body was machined from a  $\frac{1}{4}$  inch brass plate, while the dual shutter and the cover plate were machined from  $\frac{1}{8}$  inch brass plates. The 1.340 by 2.840 inch waveguide holes were all machined at the same time.

Fig. 3 is a photograph of the dual-shutter assembly with the cover plate removed in the half-closed position. Notice that a small square brass plate,  $\frac{1}{8}$  inch thick, has been inserted in the track on the main body piece, and the milled out hole for one of the waveguide openings was extended by an amount equal to the length of the inserted piece. This simple arrangement provides a mechanical stop for the shutter travel in both directions and also prevents RF leakage when the shutters are partially opened.

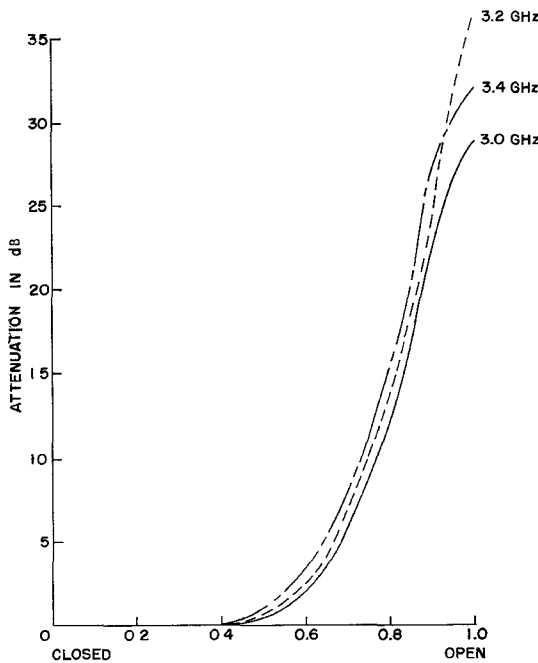


Fig. 4. Attenuation versus shutter position.

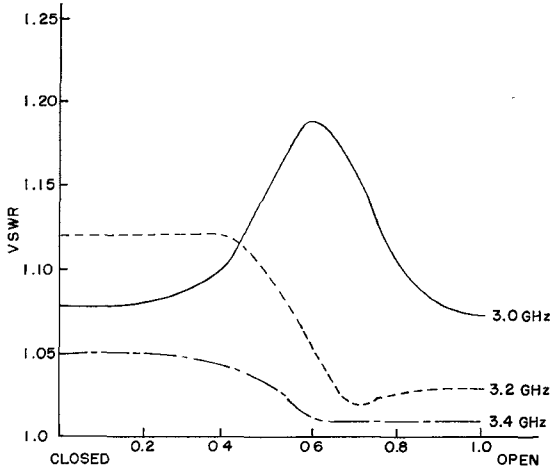


Fig. 5. VSWR versus shutter position.

The power divider has operated satisfactorily at power levels of up to 700 kW and has exhibited a dynamic range of power division in excess of 36 dB. When the RF shutters were adjusted throughout their full range of movement, operating at 200 kW peak, no visible shift in the transmitter frequency was observed.

VSWR and attenuation measurements were conducted at frequencies from 2.8 to 3.6 GHz at a 70 mW power level. The results from 3.0 to 3.4 GHz are shown in Figs. 4 and 5.

For maximum power division the power divider should be operated within the passband of the coupler. The attenuation was 34.2 dB at 3.1 GHz and 36.7 dB at 3.2 GHz, while outside the passband the maximum attenuation was only 25 dB at 3.6 GHz and 18 dB at 2.8 GHz. The VSWR remained below 1.20 over the test band. The VSWR of the loads did not exceed 1.09.

At a peak power level of 500 kW, it was

possible to vary the power output from a high value of 500 kW peak to a minimum of 160 watts peak. This is an actual high-power dynamic range of 35 dB.

Colloidal graphite powder is used to eliminate binding of the RF shutter. After 100 to 200 hours of operation, the power divider is taken apart and cleaned and lubricated. For more positive control of the power adjustment, future models will employ a rack-and-pinion or worm-gear drive. The size and weight of the device can be substantially reduced by employing commercially available adapter fittings and loads.

The basic concept for the microwave power divider described was conceived jointly by the author and F. Jellison of Microwave Associates, Inc., Burlington, Mass.

ROBERT M. TRUE  
Electronic Components Lab.  
USAECOM  
Fort Monmouth, N. J.

## Controlled Wideband Differential Phase Shifters Using Varactor Diodes

For phased array transmitting systems diode step phase shifters of limited bandwidth have been developed. Thereby PIN diodes are used because they switch high peak power with low loss. In certain receiving systems and in most microwave measurements, however, a continuous phase adjustment is required. Thus, low power analog phase shifters covering broad frequency bands are desirable. This correspondence describes an electronically-controlled three-port network using varactor diodes, which produces a constant phase difference between the two output ports.

This three-port consists of a power divider at the input and two coaxial lines, each loaded by identical series reactances at equal spacings (Fig. 1). In one of these lines the reactances are inductive, while in the other they are capacitive such that the phase versus frequency responses have equal gradients in the prescribed frequency band (Fig. 2). Thus the phase difference will be independent of frequency. The reactances are realized with varactor diodes controlled by reverse bias. The equivalent circuit of the diode mounted in series with the inner conductor of the coaxial line consists basically of an inductance in series with the diode junction capacitance. This arrangement provides positive reactance if the series resonance of the diode is below, and negative reactance if the diode resonance is above the operating frequency.

In the equivalent circuit representation at the diode in its holder, the transition from the coaxial line center conductor to the crystal is approximated by a stepped geometry [Fig. 3(a)]. Each constant diameter section ( $T_0 - T_1$ ,  $T_1 - T_2$ , etc.) is considered as a short piece of homogeneous transmission line which is sufficiently short to be represented by an equivalent series inductance and two shunt capacitances. Furthermore the stray fields excited by each diameter step are taken into account by additional shunt capacitances. The spring and crystal are represented by a lead inductance  $L_s$ , a series resistance  $R_s$ , and the junction capacity  $C_j$ . Capacitances between the facing surfaces  $T_0 - T_0'$ ,  $T_1 - T_1'$ , and  $T_2 - T_2'$  must also be considered. Numerical values of the equivalent circuit elements are such that the circuit can be simplified considerably. Thus, all shunt capacitances can be lumped into single shunt capacitances at the reference planes  $T_0$  and  $T_0'$  as shown in Fig. 3(b). In the actual networks, the values of  $L_s$  and  $C_j$  have been measured by a method similar to that given by Roberts,<sup>1</sup> whereas  $R_s$  has been determined by Crook's method.<sup>2</sup> The remaining reactances, which depend on the dimensions of the line, have been evaluated by approximation formulas<sup>3</sup> and verified experimentally.

Manuscript received March 6, 1967; revised June 1, 1967.

<sup>1</sup> D. Roberts, "Measurements of varactor diode impedance," *Trans. Microwave Theory and Techn'ques*, vol. MTT-12, pp. 471-475, July 1964.

<sup>2</sup> D. Crook, "A simplified technique for measuring high quality varactor parameters," *Solid State Design*, vol. 6, pp. 31-33, August 1965.

<sup>3</sup> C. Liechti, "Steuerbare, breitbandige Differenzphasenschieber mit Kapazitätsdioden im Mikrowellengebiet," Dissertation No. 3926, Swiss Federal Institute of Technology, Zurich, Switzerland, 1967.